CHAOS CONTROL OF ATOMIC FORCE MICROSCOPE SYSTEM USING NONLINEAR MODEL PREDICTIVE CONTROL

J. Keighobadi J. Faraji* S. Rafatnia

Department of Mechanical Engineering
University of Tabriz
Tabriz, Iran

ABSTRACT

Owing to robust and optimal specification, model predictive control method has received wide attentions over recent years. Since in certain operational conditions, an Atomic/scanning Force Microscope (AFM) shows chaos behavior, the chaos feedback control of the AFM system is considered. According to the nonlinear model of forces interacting between the tip of micro cantilever and the substrate of AFM; the nonlinear control methods are proposed. In the paper, the chaos control of a micro cantilever AFM based on the nonlinear model predictive control (NMPC) technique is presented. Through software simulation results, the effectiveness of the designed NMPC of the AFM is assessed. The simulation results together with analytical stability proofs indicate that the proposed method is effective in keeping the system in a stable range.

Keywords: Chaos, Atomic force microscope (AFM), Nonlinear model predictive control.

1. INTRODUCTION

Since the invention of AFM in 1986 by G. Binnig *et al*. it plays a significant role in different areas of science and engineering like electronics, biological, materials, chemistry, semiconductor manufacturing [1]. An AFM can be significantly effective in manufacturing many goods, including topographic three-dimensional Nano structures and precise measurement for MEMS devices [2]. Generally speaking, on the end tip of cantilever of microscope, a sharp probe is considered to scan the substrate surface of the AFM. Thereby, the performance of AFM depends on the interaction force between the substrate and the micro cantilever. The main forces which affects the AFM mechanism include mechanical contact force, capillary forces, van der Waals forces, electrostatic forces and magnetic forces. In "contact mode" measuring method of the surface forces of AFM, a photo diode measures the deflection of light perverse where a deviation micro cantilever remain in contact with the substrate. In second method known as the "tapping mode", by vibration of micro cantilever in a frequency close to its resonant frequency and considering the changes of spring parameter, the surface forces of the AFM are measured. According to the nonlinear nature of the forces acting between the probe tip and the substrate, the micro cantilever shows chaotic behavior in certain conditions of tapping mode [3]. Analysis of the chaos behavior of the AFM is an important issue which is investigated by researchers. Burnham *et al* experimentally studied the tapping mode as a single degree of freedom nonlinear system [4]. Based on Melnikov theory, the physical conditions in which chaos may occur in the system have been obtained [5, 6]. Ashhab *et al* concluded that the chaos in the AFM depends on the damping, excitation and distance parameters between the tip-sample [6]. They showed that the state feedback control is effective to eliminate the possibility of chaotic behavior. Basso *et al* simulated numerically the chaos dynamics in the same model of Ashhab *et al* [7, 8]. Lee *et al* investigated the numerical dynamic response of AFM under van der Waals force and mechanical contact between the tip and the substrate known as Derjaguin–Muller–Toporov (DMT) model [9]. By the way, a discretized single mode model of the micro cantilever was produced using Galerkin's method. Ruetzel *et al* applied Galerkin method on dynamic equations of the AFM. Furthermore, the interaction between the tip and the substrate was studied by using the potential term of Lennard - Jones. The periodic and the chaotic behavior of the AFM system has been investigated numerically in the study [10]. Experimental and theoretical works yield that the chaos behavior in the AFM may depend on many factors. The main factors include the damper, the excitation amplitude, frequency, and the average distance between the probe tip and the substrate. The chaotic behavior during AFM operation is very risky and can make false results of the experiment. Through systematic

* Corresponding author (j.faraji@tabrizu.ac.ir)

DOI : 10.1017/jmech.2016.89
Copyright © 2016 The Society of Theoretical and Applied Mechanics
https://doi.org/10.1017/jmech.2016.89 Published online by Cambridge University Press

experiments on different types of micro cantilever in different conditions, Hu and Raman showed that the dynamic response of micro cantilever AFM may bifurcate from periodic to chaotic oscillations near transition from non-contact to tapping regimens [11]. To ensure accurate performance of AFM and to eliminate the chaotic behavior in changing the operating conditions, the active controller should be used for stability considerations. Ashhab *et al* have applied the classic proportional and derivative controller on the AFM system [5]. Arjmand *et al* used nonlinear delayed feedback control method to control chaos behavior in the AFM [3]. They showed that the chaotic behavior of the AFM using the nonlinear method can be suppressed. Yamasue *et al* presented using a new method of time delay feedback control for AFM [12]. Salarieh *et al* began using delayed feedback to control the chaos in tapping mode of AFM [13]. They used the minimum entropy algorithm to obtain a feedback gain. Yau and Wang designed PD, Fuzzy logic and sliding mode control by back-stepping controllers for AFM micro cantilever [14-16]. Nozaki *et al* used the optimal linear feedback control and the state-dependent Riccati equation to control chaos of the AFM [17]. According to the studies of chaos control in the AFM, the assumption is that the exact parameters of the model are available, and the system is not under external disturbances. However, the ideal condition cannot be always provided.

In the current paper, the chaos stability of the micro cantilever AFM using the nonlinear model predictive control is presented. The proposed cost function of the NMPC consists of quadratic terms of errors between the preferred trajectory and the predicted states of the AFM system. Generally, the implementation of a real-time NMPC algorithm is difficult in practice. Since the NMPC algorithm is complex, high computational burden is requested for online optimization. However, owing to the importance of accuracy in micro/Nano scale movements, the high-level NMPC system is designed providing mathematical stability proof of the proposed NMPC. The simulation results show that the proposed method can be used to effectively suppress the chaos of AFM. The rest of paper is organized as follows: In section 2, dynamic modeling of AFM and occurrence of chaos are discussed. In section 3, using NMPC, chaos of AFM system is controlled. Conclusions are presented in section 4.

2. AFM MATHEMATICAL MODELLING

Depending on the application case, the micro cantilever system may be operated in some modes. There are generally three types of AFM imaging, non-contact mode, contact mode, and tapping mode (or intermittent). When an AFM operates in a tapping mode, the vibration amplitude of micro cantilever increases much higher than the equilibrium distance of separation between the tip and the substrate. The tapping mode AFM can be used to characterize the elastic, viscoelastic, electrical and thermal properties of a surface [2]. The tapping mode is the most widely used mode of operation, in which the motion governing dynamics is nonlinear [10]. In this paper, the non-linear dynamicsand chaos of a piezoelectric micro cantilever probe in tapping mode of the AFM will be investigated. As previously mentioned, it is necessary to simulate the dynamics of micro cantilever completely before any examination of the interaction between the AFM tip and the substrate. The physical model of the AFM in tapping mode is shown schematically in Fig. 1. The base of the micro cantilever is excited by a dither-piezo generating a displacement $\psi\cos(\omega t)$ where ψ is the amplitude of excitation and ω is excitation frequency. The micro cantilever is controlled by a piezo-actuator. The first model of micro cantilever vibration in tapping mode as a mass - spring – damper was made by Morita, Bhushan and Zhang [18, 19].

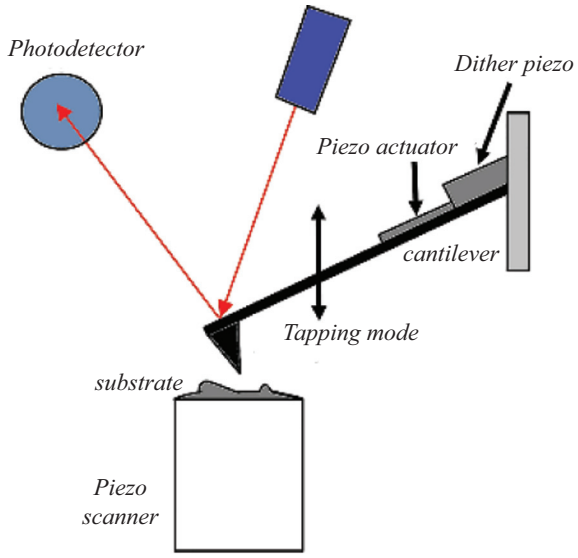


Fig. 1 Model of an AFM.

Considering merely the first mode of vibration, the cantilever is modeled as a mass - spring – damper system of Fig. 2. The cantilever is characterized with the equivalent mass, m linear spring coefficient, k and damping coefficient, c. The interaction between the cantilever and the substrate is made by the probe tip mounted to the bottom surface of the cantilever. The probe tip is modeled by a sphere of radius, R. A piezo actuator is applied to produce the input force, F_u required for the movement control of the micro cantilever. The interaction force between the cantilever tip and the surface of the substrate is considered according to the model released by Rutzel *et al* [10]. Using the potential term of the Lennard – Jones, the interaction force between the AFM tip and the substrate is represented as:

$$U_{LJ}(x,z_0)=\frac{H_1R}{1260(z_0+x)^7}-\frac{H_2R}{6(z_0+x)} \tag{1}$$

where, z_0 and x denote the AFM's tip position and displacement, respectively. H_1 and H_2 stand for Hamaker fixed parameters in the interaction between the AFM tip and the substrate regarding the potential of attraction and repulsion, respectively. The Hamaker con-

https://doi.org/10.1017/jmech.2016.89 Published online by Cambridge University Press

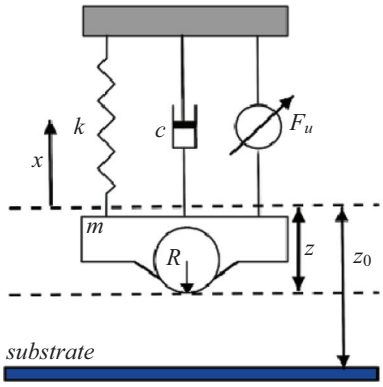


Fig. 2 Scheme of the mass- spring-damping model for the AFM cantilever vibrating.

stants are defined as $H_1 = \pi^2\rho_1\rho_2 c_1$ and $H_2 = \pi^2\rho_1\rho_2 c_2$. In Hamaker parameters, ρ_1 and ρ_2 are the densities of the two interacting components also c_1 and c_2 are the interaction constants.

When the cantilever is driven close to the substrate, three different types of forces are considerable. The first force is the spring force. The second is van der Waals attraction force which is proportional to the inverse square of the distance between the tip of cantilevers and the substrate. The third, van der Waals repulsive force is inversely proportional to the distance between the tip and substrate powered by eight. The *LJ* force is written as the summation of the repulsion and attraction forces as follows.

$$F_{LJ} = -\frac{\partial U_{LJ}(x, z_0)}{\partial (x, z_0)} = \frac{H_1 R}{180(z_0 + x)^8} - \frac{H_2 R}{6(z_0 + x)^2} \tag{2}$$

As shown in Fig. 2, the governing equation of motion of the micro cantilever is obtained:

$$m\ddot{x} + c\dot{x} + kx = F_{LJ} + \psi \cos(\omega t) + F_u \tag{3}$$

To make Eq. (3) dimensionless, the following parameters are defined:

$$T = \omega t \quad y = \frac{x}{z_s} \quad \dot{y} = \frac{\dot{x}_s}{z_s} \quad \omega = \sqrt{\frac{k}{m}} \quad a = \frac{z_0}{z_s} \quad b = \frac{c}{n\omega}$$
$$h = \frac{H_1 R}{180 m\omega^2 z_s^9} \quad d = \frac{H_2 R}{6 m\omega^2 z_s^3} \quad z_s = \frac{3}{2}\sqrt[3]{\frac{H_2 R}{3k}} \quad L = \frac{F_u}{m\omega^2 z_s} \tag{4}$$

Therefore, the following non-dimensional differential equation is resulted.

$$\ddot{y} + b\dot{y} + y - F(y) - f\cos(T) = L \tag{5}$$

Where

$$F(y) = \frac{h}{(a+y)^8} - \frac{d}{(a+y)^2} \tag{6}$$

To transform Eq. (5) to the state space system, the following two state variables, x_1 and x_2 are defined:

$$\begin{aligned} x_1 &= y \\ x_2 &= \dot{y} \end{aligned} \tag{7}$$

Hence,

$$\begin{aligned} \dot{x}_1 &= x_2 \\ \dot{x}_2 &= -bx_2 - x_1 + F(x_1) + f\cos(T) + L \end{aligned} \tag{8}$$

In Eq. (8), x_1 indicates the non-dimensional displacement of the micro-cantilever tip, T is the non-dimensional time, x_2 denotes the non-dimensional micro-cantilever tip velocity of the micro cantilever. Discretization of Eq. (8) yields as:

$$\begin{aligned} x_1(k+1) &= x_1(k) + x_2(k)\Delta T \\ x_2(k+1) &= x_2(k) + [-bx_2(k) - x_1(k) + F(x_1(k)) \\ &\quad + f\cos(T) + L]\Delta T \end{aligned} \tag{9}$$

Where, ΔT denotes the sampling time of system. In study on soft mono-crystalline silicon micro cantilever, the interaction with a flat silicon substrate is considered. The parameters of the dynamic cantilever, which are taken from a commercial AFM referred [10], are listed in Table 1.

Table 1 Properties and dimensions of the cantilever [10].

descriptions	symbol	value
length	L_1	449 μm
thickness	t_1	1.7 μm
width	w_1	46 μm
Tip radius	R	150 nm
Material density	ρ	2330 kgm^{-3}
Static stiffness	k	0.11 Nm^{-1}
Elastic modulus	E	176 GPa
1st resonance	f_1	11.804 kHz
Q factor (air)	Q	100
Hamaker (rep.)	H_1	$1.3596 \times 10^{-70} Jm^6$
Hamaker (att.)	H_2	$1.865 \times 10^{-19} J$

Hence, the numerical values of the parameters are obtained as:

$$h = \frac{9}{28}10^{-5} \quad f = 2 \quad b = 0.04 \quad d = \frac{4}{27} \quad a = 0.8 \tag{10}$$

Chaos in particular systems, is sensitive to the initial conditions. To analyze the behavior of dynamical systems and identification of chaotic responses, two well-known methods including Poincare map and maximum Lyapunov exponents are used. According to Eq. (5), considering some practical values of the parameters and also the common initial conditions like, $x_1 = 0.6$ and $x_2 = 0$, the system shows chaotic behavior [20]. By use of the aforementioned values of parameters and the initial conditions, the simulated specifications of the chaos micro-cantilever system including the movement of the AFM tip, phase portrait diagram, the Poincar´e map and the Lyapunov exponents are represented in Figs. 3, 4(a),

https://doi.org/10.1017/jmech.2016.89 Published online by Cambridge University Press

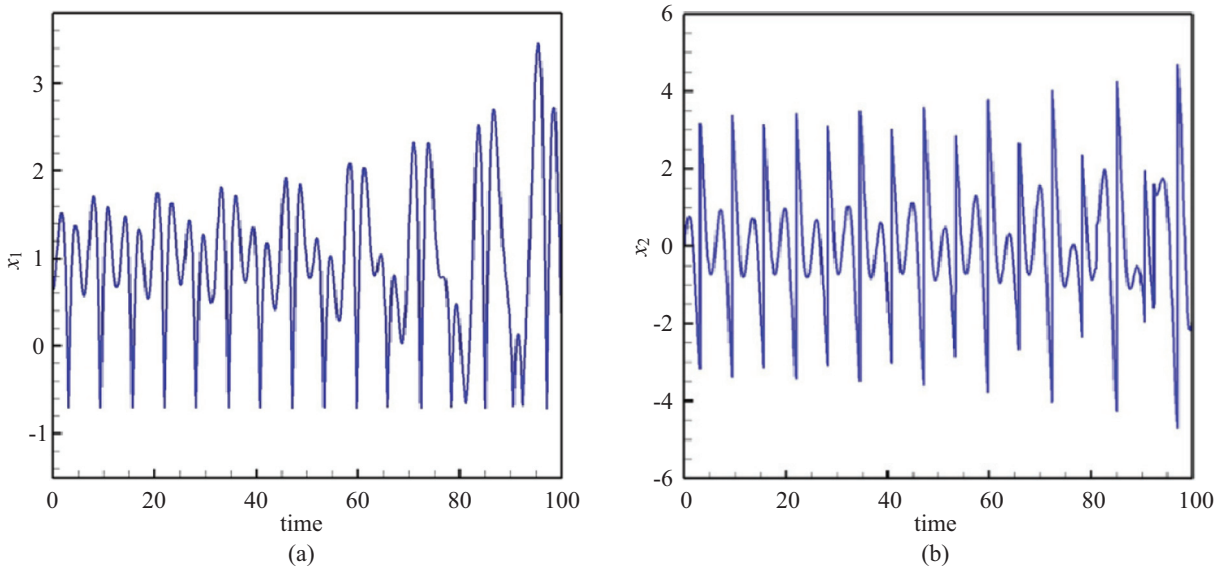


Fig. 3 (a) Micro cantilever displacement without control, (b) Micro cantilever velocity without control.

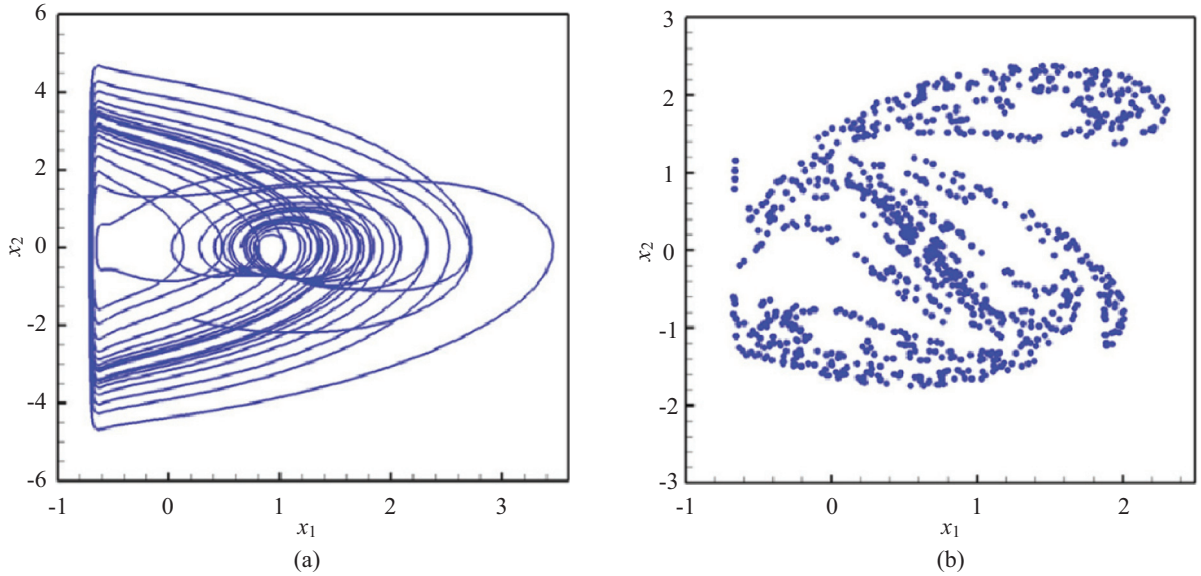


Fig. 4 Chaotic behavior in AFM with real parameters: (a) in phase space and (b) in Poincare section of 10,000 points.

4(b) and 5, respectively. According to Fig. 5, the positive maximum Lyapunov exponent depicts the expected chaotic behavior of the AFM in tapping mode operation. Since the chaotic behavior in AFM is unpleasant, a control system is designed in order to suppress the undesirable behavior.

3. CONTROL SYSTEM DESIGN

Model Predictive Control (MPC) is an effective method to control nonlinear systems. MPC can overcome the limitations of multi-input multi-output systems. It has been used in petrochemical and industrial processes with a relatively large sampling period. Recently, according to the rapid development of computers and study of numerical calculation methods, the MPC may be

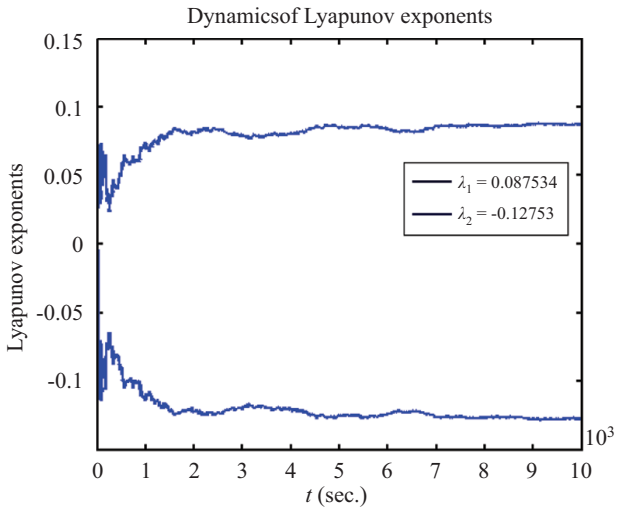


Fig. 5 Lyapunov exponents.

https://doi.org/10.1017/jmech.2016.89 Published online by Cambridge University Press

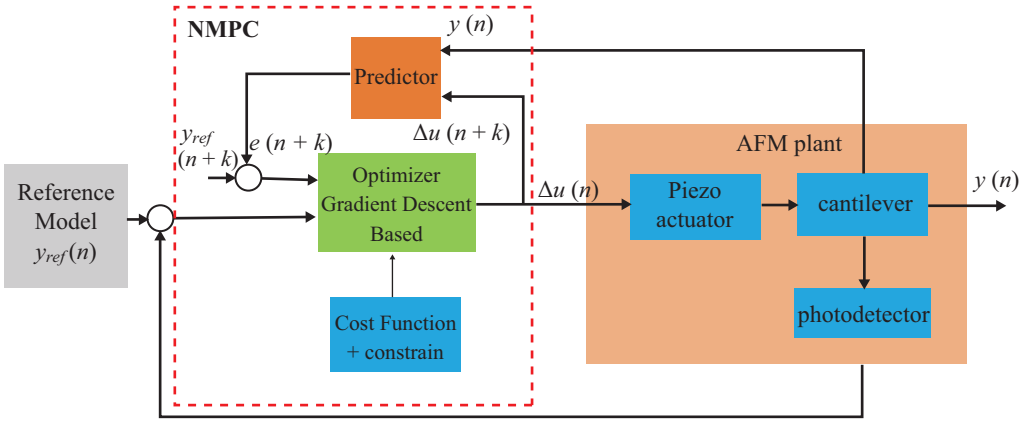


Fig. 6 AFM system basic structure using NMPC.

applied to mechanical systems with small sampling periods [21]. However, in systems which very complex samples or a shorter period is required; MPC cannot be used due to the large computational cost [22]. In these cases, common linear models are not sufficient to describe the process dynamics and nonlinear effects. Therefore, this motivates the use of nonlinear model predictive control (NMPC). To design such a high level controller, a new NMPC is used in this paper. Owing to recent developments in the speed and performance of microprocessors, the NMPC systems are going to be popular. In the NMPC, the control action is obtained by solving an optimal control problem over a finite horizon of future data. In fact, the first control input is used at the current time step, and the rest is saved as an initial condition for the online optimization at the next time step. However, with the recent increases in computational resources and the development of efficient control algorithms, the NMPC is used to control many faster systems such as submarines [23] and aircraft [24, 25]. The newly proposed NMPC is used for chaos control of AFM-TM by minimizing the state errors and tracking the reference signal. MPC is an advanced control tool which uses an internal model and predicts the future behavior of the system [26]. The NMPC's basic structure is shown in Fig. 6. It consists of a predictor block that predicts future input by minimizing a cost function in optimizer block; and AFM block, which includes the dynamic of the system. The output of AFM block is compensated with reference future trajectory that is provided from a reference model block. As shown by the practical simulation model of Fig. 6, the control action signal generated by the NMPC algorithm is received by a piezoelectric actuator. The imposed electrical control signal on piezoelectric causes cantilever's displacement which is measured by the photo diode in practice.

The advantages of the MPC can be listed as follows:

- Limited control information is required to use this control method due to a simply understanding of the principles and basic concepts and simple adjustment of its parameters.
- The MPC algorithm can be used for systems with simple or complex dynamics, with a long delay time, non-minimal phase and unstable processes.
- This algorithm essentially compensates the dead time, and can be easily used in multivariable systems.
- MPC is a feed forward control algorithm and is used to compensate measurable disturbances.
- When the output reference in future periods is known, the performance of this algorithm is very suitable.

The discretized Eq. (9) is redefined by a nonlinear state space model as:

$$x_{k+1} = f(x_k, u_k) \tag{11}$$

Subject to $x(k) \in X$, $u(k) \in U$. Where $f: R^n \times R^m \rightarrow R^n$, is a nonlinear functions vector, $x(k) \in R^n$ and $u(k) \in R^m$ represent the state and control input vectors at time k, respectively. The mismatch between the reference and predicted values can be represented by the following cost function [26].

$$J_N = \varphi(X_E(N)) + \sum_{k=0}^{N-1} \eta(X_E(k), u(k))$$
$$= \frac{1}{2} X_E^T(N) P X_E(N) + \frac{1}{2} \sum_{k=0}^{N-1} (X_E^T(k) Q X_E(k) + u_k^T R u_k) \tag{12}$$

Where, the error between reference trajectory and current state is written as, $X_E(k) = X^{ref}(k) - x_k$. The reference state vector is chosen as a sinusoidal force in standard tapping mode operation [3]. N is the length of prediction horizon. The cost function on the terminal state is specified by $\varphi(X_E(N))$. P, Q and R are weighting matrices of state error and control components, respectively. The objective is to find a feedback control law that the finite horizon cost function in Eq. (12) is minimized. According to Fig. 7, the receding time horizon of the NMPC is chosen 5 steps ($N = 5$). Consequently, when $K = 0$, the control horizon is from $K = 0$ to $K = 4$ and the predictive horizon is from $K = 1$ to $K = 5$.

3.1 Stability Analysis

The techniques used to guarantee the stability of NMPC include terminal equality constraint, terminal cost function and terminal constraint set [21]. It is well known that the stability of a finite receding horizon Eq.

https://doi.org/10.1017/jmech.2016.89 Published online by Cambridge University Press

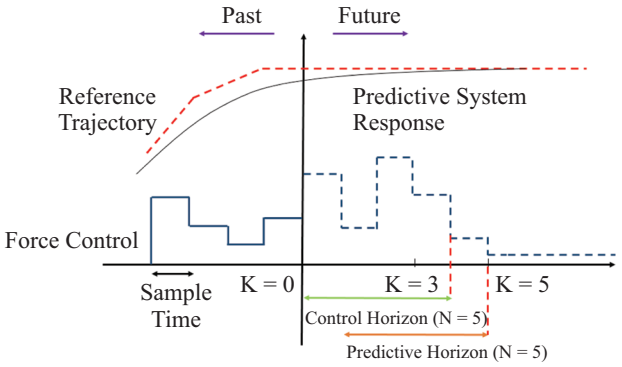


Fig. 7 A discrete nonlinear model predictive control approach.

(12) by adding a terminal state penalty term $\varphi(X_E(N))$ to this optimization problem can be guaranteed [22]. To prove the stability of NMPC for a terminal constrain set $X_0 \in X$ the following assumption is needed.

Assume 1: for each $X_E(k) \in X_0$ an acceptable control value exists $u_k(X_E(k)) \in U$ such that:

$$f(X_E, u_k(X_E)) \in X_0 \tag{13}$$

Assume 2: The terminal cost $\varphi(X_E)$ in Eq. (12) is such that for each $X_E \in X_0$ there exists an acceptable control value $u_k(X_E) \in U$ for Eq. (10) and

$$\varphi(X_E(N)) - \varphi(X_E(N-1)) + \eta(X_E(N-1), u_{N-1}) \le 0 \tag{14}$$

Assumption 2 shows that φ is a local Lyapunov function. [22].

Theorem 1: The system Eq. (11) is asymptotically stable if assumptions 1 and 2 holds.

Proof Theorem1: first, it is shown that for each $u_{N-1} \in U$ Eq. (15) can be satisfying.

$$J_N \le J_{N-1} \tag{15}$$

Using Eq. (12)

$$\begin{aligned} J_N &= \varphi(X_E(N)) + \sum_{k=0}^{N-1} \eta(X_E(k), u_k) \\ &= \varphi(X_E(N)) + \sum_{k=0}^{N-2} L(X_E(k), u_k) + \eta(X_E(N-1), u_{N-1}) \end{aligned} \tag{16}$$

Regarding $\sum_{k=0}^{N-2} \eta(X_E(k), u_k) = J_{N-1} - \varphi(X_E(N-1))$ by Eq. (14), Eq. (16) can be rewritten as:

$$\begin{aligned} J_N &= J_{N-1} \\ &+ \underbrace{\varphi(X_E(N)) - \varphi(X_E(N-1)) + \eta(X_E(N-1), u_{N-1})}_{\le 0} \le J_{N-1} \end{aligned} \tag{17}$$

If the optimal value function of problem Eq. (12) is defined as V_N then, Eq. (17) leads to:

$$V_N = \inf J_N \le \inf J_{N-1} = V_{N-1} \to V_N \le V_{N-1} \tag{18}$$

Eq. (18) shows that the optimal value function is a non-increasing function.

Assume 3: there is a function $\delta_3 \in \{\delta : R_0^+ \to R_0^+\}$ such that $\eta(X_E, u) \ge \delta_3(|X_E|_{x_{ref}})$ holds for all $X_E \in X$ and all $u \in U$, then $V_N \ge \delta_3(|x|_{x_{ref}})$.

Assume 4: there is a function $\delta_2 \in \{\delta : R_0^+ \to R_0^+\}$ such that $\varphi(X_E) \le \delta_3(|X_E|_{x_{ref}})$ holds for all $X_E \in X$, then $V_N \le \delta_2(|x_E|_{x_{ref}})$.

Proof Assume 3: By principle of optimality $V_N(X_E) = \eta(X_E, u_N) + V_{N-1}(f(X_E, u_k))$ [23]. Can be reached that $V_N(X_E) \ge \eta(X_E, u_N)$ and from Assumption 3, $V_N(X_E) \ge \eta(X_E, u_k) \ge \delta_2(|x|_{x_{ref}})$.

Proof Assume 4: Repeatedly using the inequality Eq. (18) yields. And at the end by obtaining a similar inequality to Eq. (18), for $N = 1$ Eq. (18) can be obtained.

$$\begin{aligned} &V_N(x_0) \le V_{N-1}(x_0) \le \ldots \le V_1(x_0) \\ &= \varphi(X_E(1, x_0)) \to V_N(x_0) \le \varphi(X_E(1, x_0)) \end{aligned} \tag{19}$$

So by using Assumption 4 and Eq. (19), $V_N(x_0) \le \phi(X_E(1, x_0)) \le \delta_3(|X_E|_{x_{ref}})$.

The results of Assumption 3 in conjunction with the results from assumption 4 show the asymptotic stability of NMPC [23].

In this section, the stability conditions of NMPC are explained. As shown by Eq. (14), by choosing terminal cost function as a Lyapunov function candidate, the asymptotically stable NMPC is concluded if Theorem1 be satisfied. The aforementioned condition is given as:

$$\begin{aligned} &\frac{1}{2} X_E^T(N) P X_E(N) - \frac{1}{2} X_E^T(N-1) P X_E(N-1) \\ &+ \frac{1}{2} X_E^T(N-1) Q X_E(N) + \frac{1}{2} u_{N-1}^T R u_{N-1}^T \le 0 \end{aligned} \tag{20}$$

Eq. (20) shows that the asymptotic stability is guaranteed by proper tuning, N and the weighting matrices. So the system state error converges towards zero.

For the solution of the optimal control problem, several methods exist such as Newton's method, interior point method, gradient descent method and Genetic algorithm based method. In this paper, the gradient descent method is used to solve the online optimization problem by a numerical approach.

3.2 Gradient Descent Optimization Algorithm

In this method the discretized model from Eq. (11) is added to optimization the problem Eq. (12) by using Lagrange multiplier as constrain of the problem. So the cost function from Eq. (12) is redefined after the Lagrange multiplier vector terms $\lambda_k (k = 1, \ldots, N)$ are added.

https://doi.org/10.1017/jmech.2016.89 Published online by Cambridge University Press

$$J_N = \varphi(X_E(N)) + \sum_{k=0}^{N-1} \eta(X_E(k), u(k)) + \lambda_{k+1}^T [f(x_k, u_k) - x_{k+1}] \tag{21}$$

If the Hamiltonian function is defined as: $H_k = \eta(X_E(k), u_k) + \lambda_{k+1}^T f(x_k, u_k)$, Eq. (21) is rewritten by Eq. (22).

$$\begin{aligned} J_N &= \varphi(X_E(N)) + \sum_{k=0}^{N-1} (H_k - \lambda_{k+1}^T f(x_k, u_k) + \lambda_{k+1}^T [f(x_k, u_k) - x_{k+1}] \\ &= \varphi(X_E(N)) + \sum_{k=0}^{N-1} (H_k - \lambda_{k+1}^T x_{k+1}) \\ &= \varphi(X_E(N)) - \lambda_N^T x_N + \sum_{k=0}^{N-1} (H_k - \lambda_k^T x_k) \end{aligned} \tag{22}$$

The differentiation of the cost function Eq. (22) yields as:

$$\begin{aligned} dJ = &\left[\frac{\partial \varphi(X_E(N))}{\partial x} - \lambda_N^T \right] dx_N \\ &+ \sum_{k=0}^{N-1} \left[\left(\frac{\partial H_k}{\partial x_k} - \lambda_k^T \right) dx_k + \frac{\partial H_k}{\partial u_k} du_k \right] \end{aligned} \tag{23}$$

If the Lagrange multipliers are chosen as

$$\lambda_N^T = \frac{\partial \varphi(X_E(N))}{\partial x_N} \quad \text{and} \quad \lambda_N^T = \frac{\partial H_k}{\partial x_k} \tag{24}$$

The differential change of the cost function is simplified to:

$$\partial J = \sum_{k=0}^{N-1} \frac{\partial H_k}{\partial u_k} du_k \tag{25}$$

Using Hamiltonians supposed function, the gradient of the function in respect to the control input can be written as:

$$\frac{\partial H_k}{\partial u_k} = \frac{\partial L(X_E(k), u_k)}{\partial u_k} + \lambda_{k+1}^T \frac{\partial f(x_k, u_k)}{\partial u_k} \tag{26}$$

For decreasing gradient of cost function, the next control input should be in negative direction of Eq. (26).

$$u_{k+1} = u_k - \rho \frac{\partial H_k}{\partial u_k} \quad (0 < \rho < 1) \tag{27}$$

The steps of the designed optimization algorithm are organized as Fig. 8. The steps will be repeated until the sampling time ends.

4. SIMULATION AND RESULTS

In section 3, the nonlinear model predictive control has been designed to control chaos phenomenon in the AFM. Considering the numerical values given by Eq. (10) and initial conditions, $x_1 = 0.6$ and $x_2 = 0$, the system is confronted to chaos. The phase plane of the

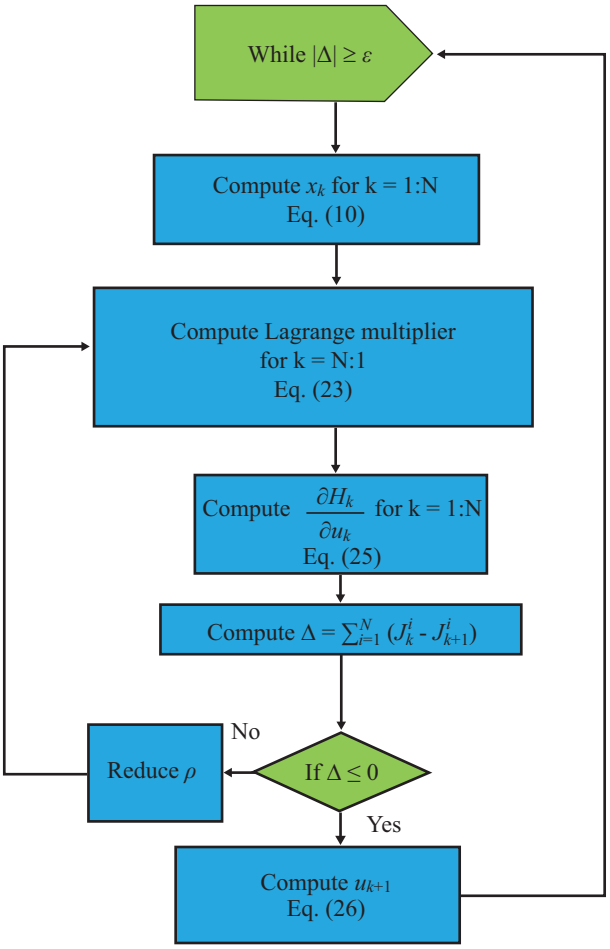


Fig. 8 Gradient descent optimization algorithm.

AFM with Eq. (9) and without feedback control was shown in Fig. 4(a). The sinusoidal reference trajectory for the displacement is used as, $x_{d1} = 0.6\sin(T)$ and $x_{d2} = 0.6\cos(T)$. Table 2 shows the parameters used in the simulation.

Table 2 Conditions of AFM system.

Initial x_0	$[0.6,0]^T$
Initial u_0	0
Weight matrix **P**	diag $[0.1,0.1]^T$
Weight matrix **Q**	diag $[18,18]^T$
Weight matrix **R**	0.1
Sampling period	0.001 [s]
Time delay by calculation	0.001 [s]

4.1 Simulation without Noise

As the simulation results show in Figs. 9 through 11, the feedback control is activated at $t = 50\ s$. In Fig. 9, the displacement and velocity of the micro cantilever following the application of NMPC system are shown. The control force regarding the stability of the AFM system is shown in Fig. 10. Figure 11 shows the phase plane after the force control.

https://doi.org/10.1017/jmech.2016.89 Published online by Cambridge University Press

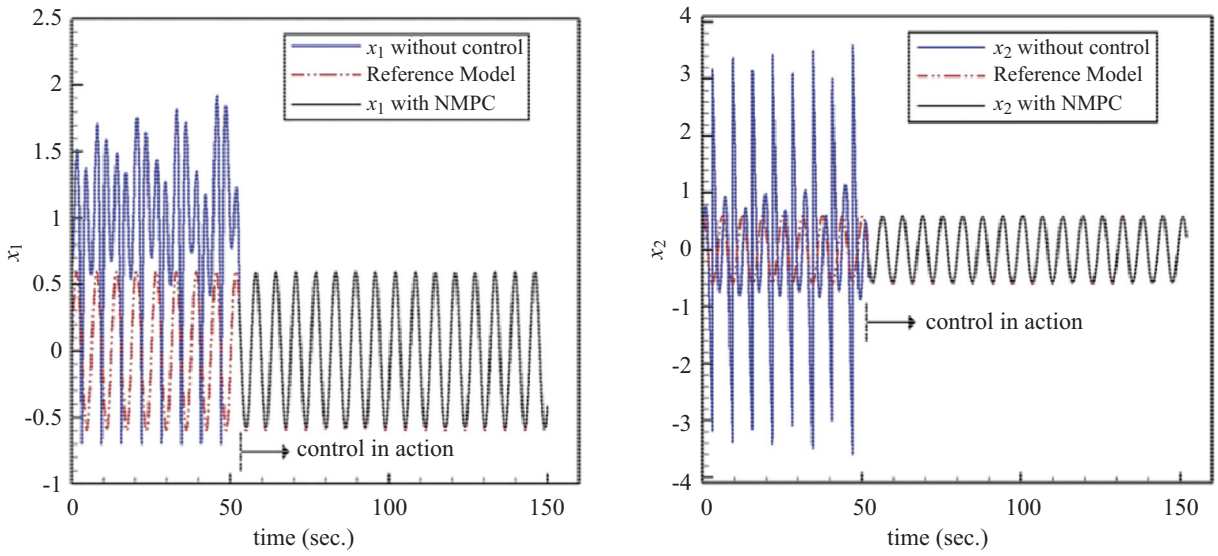


Fig. 9 Displacement and velocity of the micro cantilever based on NMPC.

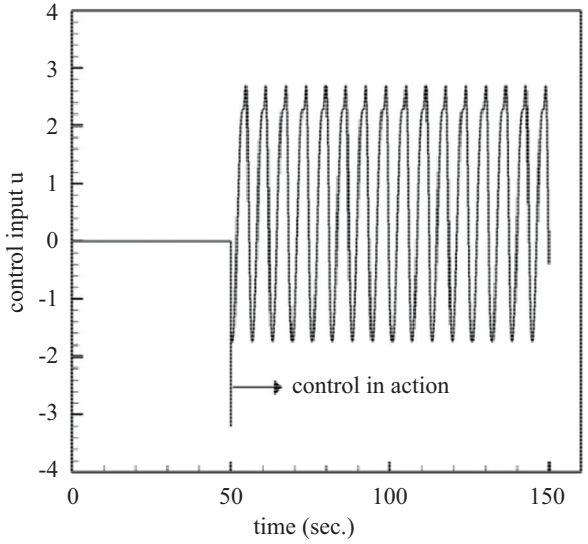


Fig. 10 Control effort force of NMPC without noise.

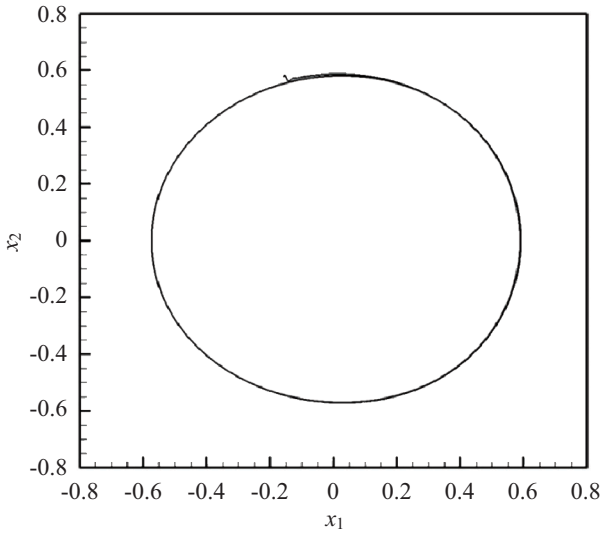


Fig. 11 Phase plane using NMPC without noise.

4.2 Comparison with Linear Feedback Control and NMPC

To assess the performance of the proposed NMPC method that applied to an AFM, the controlled non-dimensional displacement and velocity of the cantilever tip through a linear feedback control (LFC) algorithm are represented. The error dynamics of control system is rewritten as the following error model [27].

$$\begin{aligned}\dot{e}_1 &= e_2\\ \dot{e}_2 &= -be_2 - e_1 + \frac{h}{(b+e_1+x_1^*)^8} - \frac{h}{(b+x_1^*)^8} - \frac{d}{(b+e_1+x_1^*)^2}\\ &\quad + \frac{d}{(b+x_1^*)^2} + u_{of}\end{aligned} \tag{28}$$

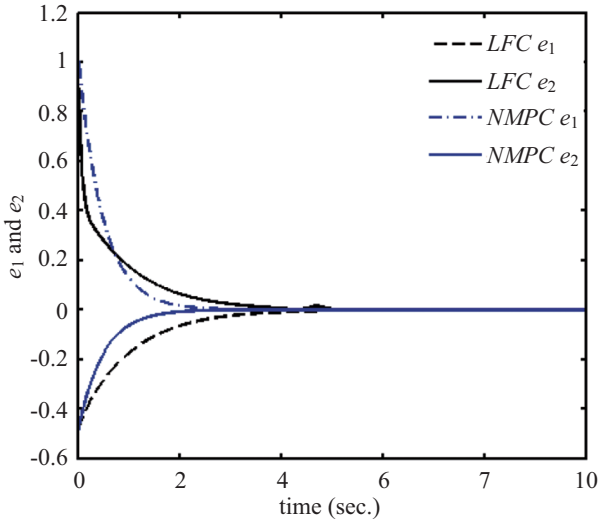


Fig. 12 Comparison of displacement and velocity tracking errors between NMPC and LFC methods.

https://doi.org/10.1017/jmech.2016.89 Published online by Cambridge University Press

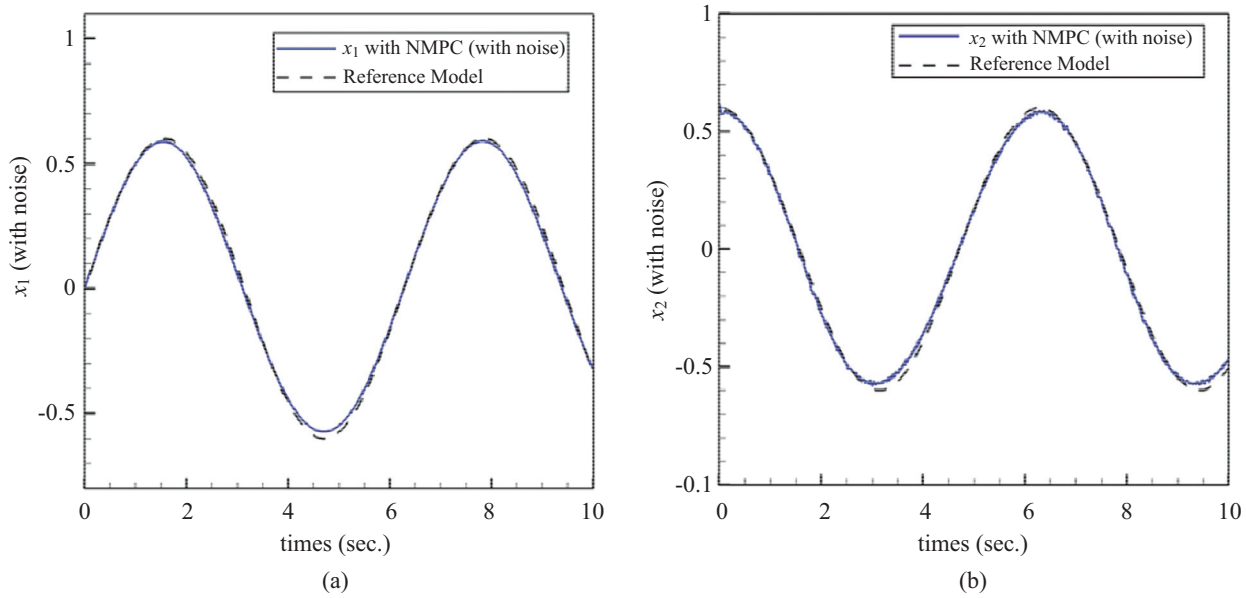


Fig. 13 Displacement and velocity of micro cantilever using NMPC under white noise.

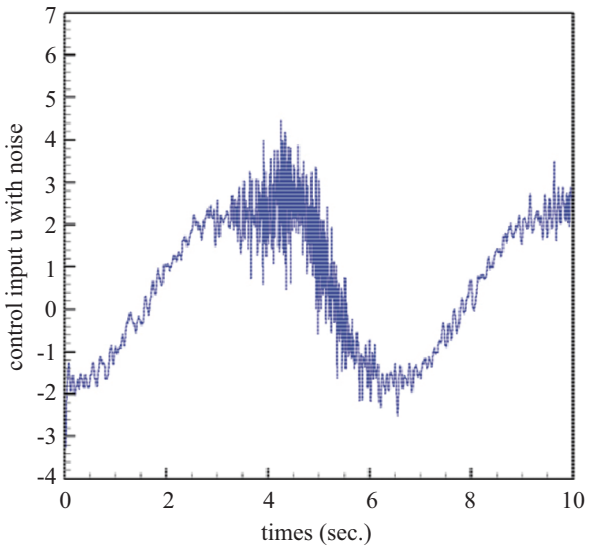


Fig. 14 Force control of NMPC together with white noise.

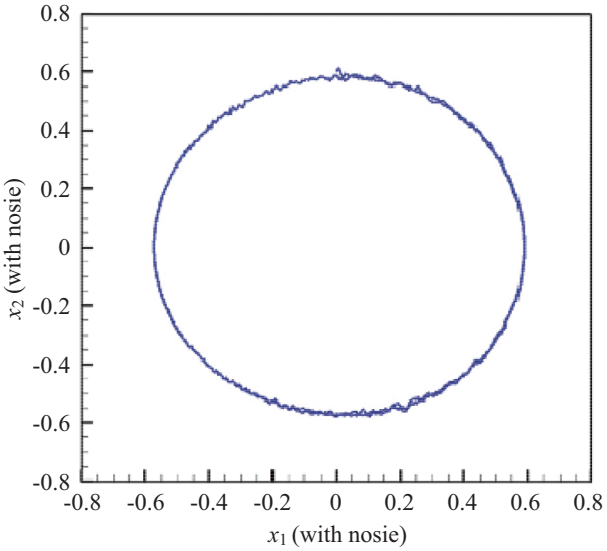


Fig. 15 Phase plane considering the NMPC together with white noise.

Where x^* and u_{of} are the desired periodic orbit and the feedback control force respectively; $e = [e_1 \quad e_2]^T$ stands for the deviation from the desired orbit ($e = x - x^*$). The LFC algorithm is applied on the continuous time nonlinear dynamic system of Eq. (28). Figure 12 shows the performance of the NMPC based method compared to the LFC algorithm.

As is clear by Fig. 12, compared to the LFC method, the NMPC method results is a better performance in particular a smaller settling time.

4.3 Simulation with Noise

Through imposing random white noise on measured state variables, the simulations in 4.1 and 4.2 sections are performed in the time interval between $t = 0$ (s) and $t = 10$ (s). Figure 13 represents the displacement and the velocity states of the micro cantilever using noisy measurements in the NMPC. The control force for the stability of the AFM system in the presence of noise is shown in Fig. 14. The phase plane plot under the control force is shown in Fig. 15.

5. CONCLUSIONS

According to the widespread uses of AFM in past several years, for topography, Nano/micro manipulation, etc., there exist chaos performances. Generally speaking, the AFM is highly sensitive to chaos. Therefore, design of a feedback control system that can block the probable chaos in manufactured present AFMs without

https://doi.org/10.1017/jmech.2016.89 Published online by Cambridge University Press

hardware corrections is of utmost importance. In this paper, the chaos control in the tapping mode of AFM has been studied. By use of computer simulation, it was shown that under certain real conditions and real parameters, chaotic behavior occurs in the AFM. In order to suppress chaos and keep the system in the stable range, a NMPC strategy was used. As the main practical result without changing the physical structure of currently working AFMs, merely by implementation of newly proposed control system on the digital micro-controller of the AFM system, the chaos could be suppressed. In preceding research papers to remove the chaos of AFM, some control systems were proposed based on past time feedback errors. However, by prediction of future states and thereafter adaptation of the proportional control law, the proposed NMPC method results in a smoother and optimal performance. The small bounded control input of the NMPC makes its implementation more feasible in real AFM systems in which the actuator system could not be enhanced. The NMPC considers a model based prediction of future outputs and an optimization algorithm according to the future, current and past inputs and outputs/states of system. The optimization cost function was formulated as a mismatch between reference and predicted values of outputs and input control signals. Therefore, the computational burden of optimization algorithm is suitable for the practical AFM implementation in online. As a matter of fact, the proposed online NMPC system is significant for current and future real AFM implementations. The robustness against stochastic noises in addition to the NMPC's optimal and adaptive predictive solution, showed another practical specification of the proposed technique. Analysis of simulation results depicted that the proposed control method is very effective since the chaos trajectory has been thoroughly changed to a regular line. In the proposed control method, the convergence error of the system was very convenient. For the stability of Lyapunov sense, considering the cost function of NMPC as Lyapunov function candidate it was shown that the asymptotic stability is guaranteed by proper tuning of the receding time horizon and the weighting matrices. In online solution of optimal predictive control problem, through gradient descent method a discrete-time model of AFM was gathered to the optimization algorithm as constraint. Hence, a fast minimization control algorithm is obtained which is important in the practical AFM implementation. By inspection of the simulation results, it can be concluded that the NMPC algorithm yielded a good performance for chaos control of AFM within an acceptable range of precision of commercial AFMs.

REFERENCES

1. Xie, H., Onal, C., Régnier, S. and Sitti, M., *Atomic Force Microscope Based Nanorobotics, modelling, simulation, setup building and experiments series,* **71**, Springer, Berlin (2011).
2. Jalili, N. and Laxminarayana, K., "A review of atomic force microscopy imaging systems: application to molecular metrology and biological sciences," *Mechatronics*, **14**, pp. 907-945 (2004).
3. Arjmand, M. T., Sadeghian, H., Salarieh, H. and Alasty, A., "Chaos control in AFM systems using nonlinear delayed feedback via sliding mode control," *Nonlinear Analysis: Hybrid Systems*, **2**, pp. 993-1001 (2008).
4. Burnham, N. A., Kulik, A. J., Gremaud, G. and Briggs, G. A. D., "Nanosubharmonics: the dynamics of small nonlinear contacts," *Physical Review Letters*, **74**, pp. 5092-5095 (1995).
5. Ashhab, M., Salapaka, M. V., Dahleh, M. and Mezić, I., "Dynamical analysis and control of microcantilevers," *Automatica*, **35**, pp. 1663-1670 (1999).
6. Ashhab, M., Salapaka, M. V., Dahleh, M. and Mezić, I., "Melnikov-based dynamical analysis of microcantilevers in scanning probe microscopy," *Nonlinear Dynamics*, **20**, pp. 197-220 (1999).
7. Basso, M., Giarre, L., Dahleh, M. and Mezić, I., "Numerical analysis of complex dynamics in atomic force microscopes. in Control Applications, " *International Conference on Control Applications*, Trieste, Italy (1998).
8. Basso, M., Giarre, L., Dahleh, M. and Mezic, I., "Complex dynamics in a harmonically excited Lennard-Jones oscillator: Microcantilever-sample interaction in scanning probe microscopes," *Journal of Dynamic Systems, Measurement, and Control*, **122**, pp. 240-245 (2000).
9. Lee, S. I., Howell, S. W., Raman, A. and Reifenberger, R., "Nonlinear dynamic perspectives on dynamic force microscopy," *Ultramicroscopy*, **97**, pp. 185-198 (2003).
10. Rützel, S., Lee, S.I. and Raman, A., "Nonlinear dynamics of atomic–force–microscope probes driven in Lennard–Jones potentials," *Proceedings of the Royal Society of London A: Mathematical, Physical and Engineering Science*s, **459**, pp. 1925-1948 (2003).
11. Hu, S. and Raman, A., "Chaos in atomic force microscopy," *Physical Review Letters*, **96**, pp. 036107-036180 (2006).
12. Yamasue, K. and Hikihara, T., "Control of microcantilevers in dynamic force microscopy using time delayed feedback," *Review of Scientific Instruments*, **77**, pp. 053703-053708 (2006).
13. Salarieh, H. and Alasty, A., "Control of chaos in atomic force microscopes using delayed feedback based on entropy minimization," *Communications in Nonlinear Science and Numerical Simulation*, **14**, pp. 637-644 (2009).
14. Wang, C.-C. and Yau, H.-T., "Chaotic analysis and control of micro cantilevers with PD feedback using differential transformation method," *International Journal of Nonlinear Sciences and Numerical Simulation*, **10**, pp. 425-444 (2009).

https://doi.org/10.1017/jmech.2016.89 Published online by Cambridge University Press

15. Yau, H.-T. and Wang, C.-C., "Dynamics analysis and fuzzy logic controller design of atomic force microscope system with uncertainties," *Journal of Optoelectronics and Advanced Materials*, **11**, pp. 1178-1184 (2009).
16. Wang, C.-C., Pai, N.-S. and Yau, H.-T., "Chaos control in AFM system using sliding mode control by backstepping design," *Communications in Nonlinear Science and Numerical Simulation*, **15**, pp. 741-751 (2010).
17. Nozaki, R. *et al*., "Nonlinear control system applied to atomic force microscope including parametric errors," *Journal of Control, Automation and Electrical Systems*, **24**, pp. 223-231 (2013).
18. Morita, S., Wiesendanger, R. and Meyer, E., *Noncontact Atomic Force Microscopy*, 1, Springer, Berlin (2002).
19. Zhang, W. M., Meng, G., Zhou, J. B. and Chen, J. Y., "Nonlinear dynamics and chaos of micro cantilever-based TM-AFMs with squeeze film damping effects," *Sensors*, **9**, pp. 3854-3874 (2009).
20. Balthazar, J.M., Tusset, A.M. and Bueno, A.M., "TM-AFM nonlinear motion control with robustness analysis to parametric errors in the control signal determination," *Journal of Theoretical and Applied Mechanics*, **52**, pp. 93-106 (2014).
21. Hosseini-Pishrobat, M. and Keighobadi, J., "Force-balancing model predictive control of MEMS vibratory gyroscope sensor," *Proceedings of the Institution of Mechanical Engineers, Part C: Journal of Mechanical Engineering Science*, DOI: 10.1177/0954406215607899 (2015).
22. Chen, H. and Allgower. F., "A quasi-infinite horizon nonlinear model predictive control scheme with guaranteed stability," *Control Conference (ECC)*, Brussels, Belgium (1997).
23. Grüne, L. and Pannek, J., *Nonlinear Model Predictive Control*, Springer, London, (2011).
24. Kim, H.J., Shim, D.H. and Sastry. S., "Nonlinear model predictive tracking control for rotorcraft-based unmanned aerial vehicles," *American Control Conference*, Anchorage, Alaska (2002).
25. Slegers, N., Kyle, J. and Costello, M., "Nonlinear Model Predictive Control Technique for Unmanned Air Vehicles," *Journal of Guidance, Control, and Dynamics*, **29**, pp. 1179-1188 (2006).
26. Allgöwer, F. and Zheng, A., *Nonlinear Model Predictive Control*, **26**, Birkhäuser, Basel (2012).
27. Nozaki, R., *et al*. "COMPARISONS BETWEEN MODELING AND CONTROL METHOD APPLIED TO AN ATOMIC FORCE MICROSCOPE," *Proceedings of the 22nd International Congress of Mechanical Engineering (COBEM)*, Ribeirão Preto, Brazil (2013).

(Manuscript received March 3, 2016,
accepted for publication July 21, 2016.)

https://doi.org/10.1017/jmech.2016.89 Published online by Cambridge University Press

https://doi.org/10.1017/jmech.2016.89 Published online by Cambridge University Press